International Journal of Steel Structures
https://doi.org/10.1007/s13296-020-00377-7

Online ISSN 2093-6311
Print ISSN 1598-2351

Modified Low-Cycle Fatigue Estimation Using Machine Learning for Radius-Cut Coke-Shaped Metallic Damper Subjected to Cyclic Loading

Jaehoon Bae[1] · Chang-Hwan Lee[2] · Minjae Park[1] · Robel Wondimu Alemayehu[1] · Jaeho Ryu[3] · Young K. Ju[1]

Received: 24 January 2020 / Accepted: 5 July 2020

Abstract
In this study, a coke-shaped steel damper that exhibits in-plane resistance is introduced as a passive damper. The double-coke damper presented in this study applies the concept of reduced beam sections to increase the ductility in the case of a prolonged earthquake. Multiplastic hinges are placed on each strip by setting the radius-cut section. The fatigue performance of the damper during earthquake loading is verified through a constant cyclic loading test. The results indicate that, as the number of plastic hinges inside the strip increases, the damper ductility increases, producing a stable hysteresis graph. In addition, a new equation that considers the damage index using parameters such as maximum strength and effective stiffness is proposed, and the experimental results are found to be in excellent agreement with the number of failure cycles obtained from the proposed model. By comparing the results of applying the proposed equation with the machine learning results, it is demonstrated that machine learning can be used for estimating the damper performance against the fatigue of the resistive cycle.

Keywords Plastic hinge · Passive damper · Low-cycle fatigue · Machine learning

1 Introduction

The effectiveness of various types of passive dampers in minimizing the damage from earthquakes has been verified by many researchers (Chen et al. 2001; Tse et al. 2012; Bae and Karavasilis 2018; Christopoulos et al. 2006; Constantinou et al. 1998; Deng et al. 2015). Among them, metallic dampers are commonly used as energy-dissipation devices against earthquake loading, owing to their cost-effectiveness and ease of application. Metallic dampers can be divided into two types depending on their behavior characteristics—out-of-plane deformation-type dampers and in-plane deformation-type dampers. ADAS (Added Damping and Stiffness) and TADAS (Triangular-plate Added Damping and Stiffness) steel dampers can be categorized as out-of-plane deformation-type dampers (Khazaei 2013; Mohammadi et al. 2017). On the other hand, the cantilever-type damper with a high elastic stiffness proposed by Kim et al. (2016), and the slit damper tested by Chan and Albermani (2008), Oh et al. (2009), for verifying seismic performance are examples of in-plane deformation-type dampers.

Steel dampers dissipate energy after yielding by exhibiting plastic deformation. Therefore, the fatigue capacity of steel dampers during an earthquake is significant for the sustainable use of the damper. Low-cycle fatigue is mainly associated with cracking or fracturing of the metals under repeated fatigue with small loading and is primarily determined using strain-based methods. Additionally, steel is homogeneous, and a low-cycle fatigue-prediction equation based on plastic deformation is mainly used for determining cracking and fracturing of metals (Lee et al. 2014; Krawinkler and Zohrei 1983; Tamai et al. 1998). Fatigue prediction models for low cycles have been proposed by various researchers (Fatemi and Yang 1998; Kuroda 2002; Zhang et al. 2013). Among these models, the Mason–Coffin and

✉ Young K. Ju
tallsite@korea.ac.kr

[1] School of Civil, Environmental, and Architectural Engineering, Korea University, 145 Anam-ro, Seongbuk-gu, Seoul 02841, Republic of Korea

[2] Department of Architectural Engineering, Pukyong National University, 45 Yongso-ro, Nam-gu, Busan 48513, Republic of Korea

[3] Technical Research Center, TechSquare Co. Ltd., 25 Banpo-daero, Seocho-gu, Seoul 06710, Republic of Korea

Published online: 09 July 2020

Palmgren–Miner models have been applied widely. Lee et al. (2014) proposed a modified fatigue model for the hourglass-shaped steel strip damper, considering the total deformation and effective stiffness. Usami et al. (2011) conducted a low-cycle experiment to improve the fatigue capacity of buckling-restrained braces. They reported that the inelastic deformation relatively influenced the in-plane gap between filler members.

The COKE damper introduced in this paper is intended to induce bending deformation by adjusting the strip depth to length ratio to maximize the inelastic deformation ability due to multi hinge creation, using the concept of reduced beam section (RBS; Engelhardt et al. 1996). A constant loading test is performed to verify the fatigue performance against constant low cyclic loading. In addition, a novel modified model that considers the effects on both the overall deformation and effective stiffness, revised from the Mason–Coffin equation, is developed. The tests results show that the proposed model satisfactorily predicts the number of cycles at which fracture occurs under low-cycle fatigue. Furthermore, machine learning is used to estimate the damage index, which is then compared with the values calculated using the proposed model. The results demonstrate the possibility of utilizing machine learning in assessing the low-cycle fatigue performance with an error rate below 10%.

2 Radius-Cut Coke-Shaped Strip Damper

Figure 1 illustrates the configuration of a coke-shaped damper that shows the in-plane direction resistance and radius-cut section at the $h/8$ and $h/4$ positions from the end of the strip. The height (h)–width (b) ratio of the strip is selected to be over 5, which indicates flexural deformation rather than shear deformation (Lee et al. 2016a, b, c) is likely to occur. The fixed part is connected using frames with high-strength bolts, and the shape of the central part utilizes a moment distribution and intentionally concentrates the stress in the radius-cut section. Thus, the occurrence of multiple plastic hinges, when assuming efficient plastic deformation, is expected.

Figure 2 shows the details of the design procedure of the coke-shaped damper, which is mentioned below:

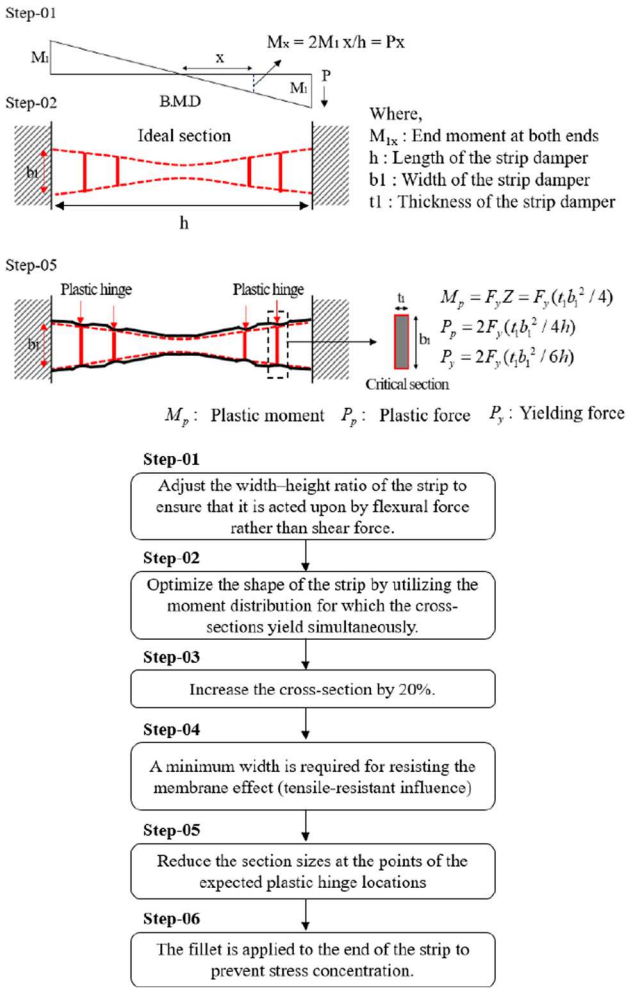

Fig. 2 Coke-shaped damper design procedure

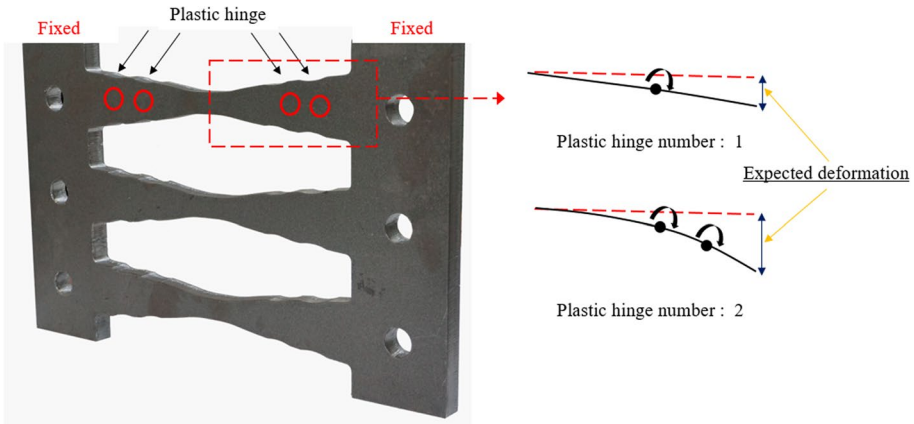

Fig. 1 Coke-shaped damper configuration

Table 1 Test specimens

Specimens	Material	Thickness (mm)	Width (mm)	Height (mm)	No. of steel plates (EA)	Plastic hinge (EA)	Loading protocol
COKE4B1	SS275	19	45	270	2	4	Constant (62 mm)
COKE4B2	SS275	19	45	270	2	4	Constant (62 mm)
COKE4B3	SS275	19	45	270	2	4	Constant (44.5 mm)
COKE4B4	SS275	19	45	270	2	4	Constant (26.5 mm)
COKE2B1	SS275	19	45	270	2	2	Constant (62 mm)
COKE2B2	SS275	19	45	270	2	2	Constant (62 mm)

Step 1 Adjust the width–height ratio of the strip to ensure that it is acted upon by flexural force rather than shear force. The moment distribution of the strip at both fixed conditions suggest a linear increase, by representing a fixed moment M_1 at both ends.
Step 2 Optimize the shape of the strip by utilizing the moment distribution for which the cross-sections yield simultaneously.
Step 3 Increase the cross-section by 20%.
Step 4 Although the effect of the shear force is small, a minimum width is required for resisting the membrane effect (tensile-resistant influence) in case a large plastic deformation occurs.
Step 5 Reduce the section sizes at the points of the expected plastic hinge locations, that is, $h/4$ and $h/8$, from the strip end by making the strip narrow gradually.
Step 6 The fillet is applied to the end of the strip to prevent stress concentration.

The theoretical strength of the damper is determined at the plastic hinge location and calculated using the plastic section modulus stated in Fig. 2.

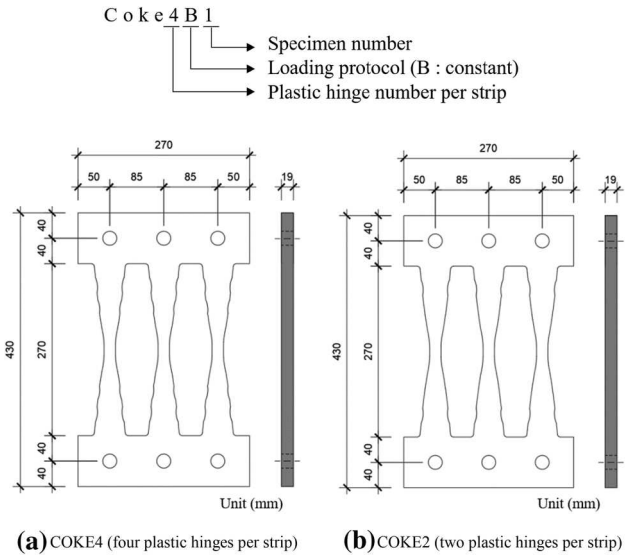

Fig. 3 Test specimens

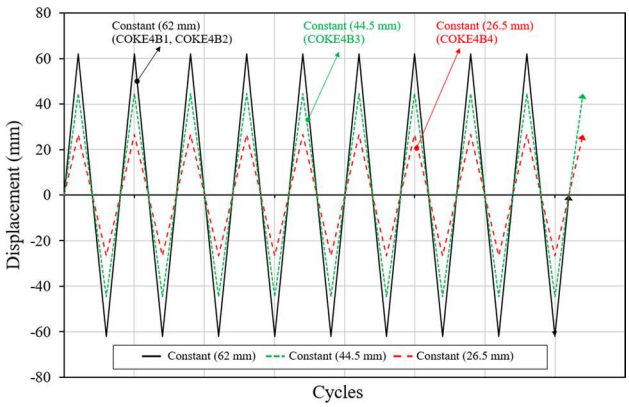

Fig. 4 Loading protocol

3 Experimental Program

3.1 Test Specimens

The specimen properties are listed in Table 1, and the details of the specimens are depicted in Fig. 3. The tests are classified into two types, based on the number of plastic hinges in a strip. COKE4 forms four plastic hinges in a strip, whereas, COKE2 forms two plastic hinges.

3.2 Loading Protocol

The cyclic force was developed using three protocols, to evaluate the fatigue repeatability of the coke damper against low-cycle fatigue. Constant loads of the same amplitude were applied through displacement control, corresponding to the target displacement (2/3 of the target

displacement, and 1/3 of the target displacement). The loading protocol used in this study is shown in Fig. 4.

3.3 Experiment Setup

Figure 5 shows the specimen setting with the dampers. An actuator of 1000 tons is used in the experiment, and a strip damper is placed between the left and right jigs to be

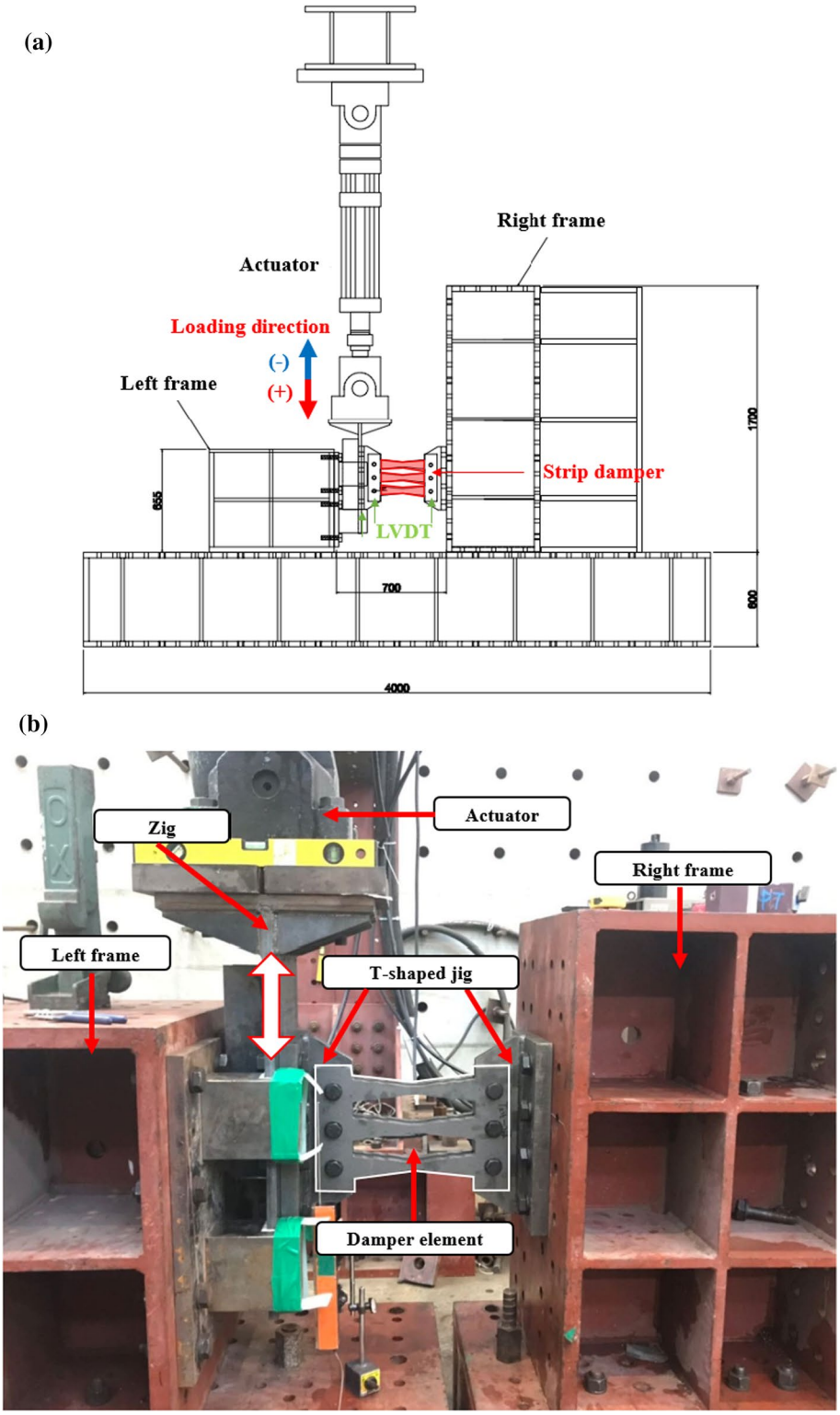

Fig. 5 Experimental details and setup

Table 2 Steel tensile test results

Specimen	B (mm)	t (mm)	Yield stress (MPa)	Tensile stress (MPa)	Yield ratio	Elongation (%)
Mean (1–3)	200.1	18.87	341	515	0.66	23.3
19t (1)	200.2	19.10	335	507	0.66	23.0
19t (2)	200.0	18.87	335	514	0.65	23.5
19t (3)	200.0	18.65	353	523	0.67	23.5

Table 3 Experimental comparison of the test results and theoretical strength

Specimen	F_{yn} (MPa)	F_{yt} (MPa)	P_{max} (kN)	P_{pn} (kN)	P_{pt} (kN)	P_{max}/P_{pn}	P_{max}/P_{pt}
COKE4B1	265.0	341.0	249.5	113.3	145.8	2.20	1.71
COKE4B2	265.0	341.0	247.1	113.3	145.8	2.18	1.69
COKE4B3	265.0	341.0	216.2	113.3	145.8	1.91	1.48
COKE4B4	265.0	341.0	181.3	113.3	145.8	1.60	1.24
COKE2B1	265.0	341.0	252.7	113.3	145.8	2.23	1.73
COKE2B2	265.0	341.0	256.5	113.3	145.8	2.26	1.76

F_{yn}, nominal yield strength; F_{yt}, material test yield strength; P_{max}, experimental result at maximum strength; P_{pn}, theoretical plastic strength based on nominal yield strength; P_{pt}, theoretical plastic strength based on test yield strength

loaded in the in-plane direction. The damper is fitted perfectly between the left and right fixing bolts, and the setting minimized the generation of surrounding moments such that the entire actuator load could flow directly into the damper.

3.4 Material Properties

No. 1A (KS B 0801) specimens were used for the tensile tests that were conducted according to the procedures of KS B 0802. As can be seen from Table 2, SS275 steel was used, and test results exceed the lower yield strength limit (265 MPa) of SS275 specified in KS D 3503.

4 Experiment Results

Table 3 presents a comparison of the experimental and theoretical strength values. From the experimental results, it was confirmed that the tested load was significantly higher than the calculated theoretical load, based on the yield strength or actual material strength. A possible reason for this difference is that the load tends to increase more than expected, because of the tensile resistance effect caused by the large stresses caused by tight fixing at both strip ends.

4.1 Load–Displacement Relationships

The load–displacement relationships of the strip damper are displayed in Fig. 6, where the drift ratio (δ/h, %) shows the overall deformation of the strip damper. Figure 6 also indicates that all the experiments using COKE4 and COKE2

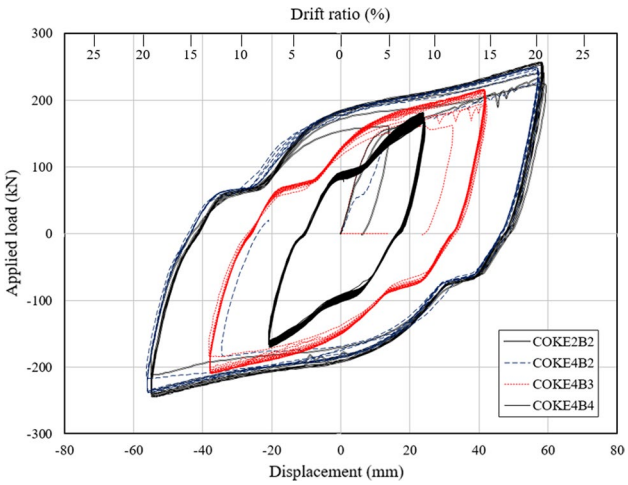

Fig. 6 Load–displacement relationships

exhibit a stable hysteresis behavior under constant load conditions.

The yielding displacement and yielding force are 4.43 mm and 53.66 kN, respectively, for COKE4B2, and 6.62 mm and 97.45 kN, respectively, for COKE2B2. As the number of plastic hinges increases, the yield point of the coke-shaped damper tends to occur sooner because of the cross-sectional defects. Figure 7 shows the ductility ratio comparisons of COKE4B2 with COKE2B2, and Fig. 8 presents the applied load variation for every cycle. In both graphs, the maximum force is higher for COKE2 damper (two plastic hinges per strip) than that for COKE4 damper (four plastic hinges per strip) in terms

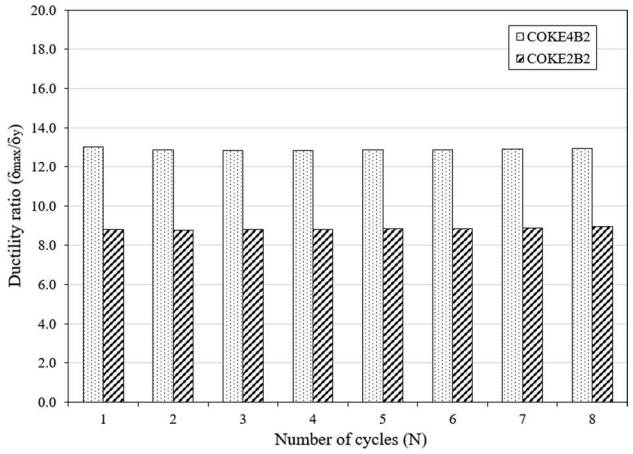

Fig. 7 Ductility ratio (δ_{max}/δ_y) versus number of cycles (N)

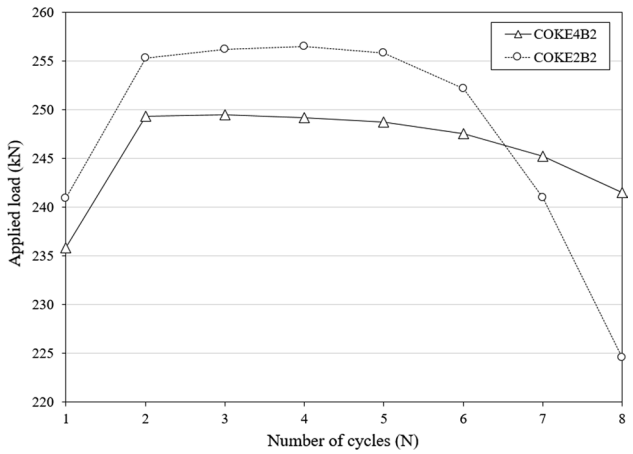

Fig. 8 Applied load variations versus number of cycles (N)

of the maximum shear resistance. However, COKE4B2 shows more progressive ductility than COKE2B2, as the maximum strength drops smoothly by approximately 4% from the maximum force, exhibiting a drop of 13% from the maximum force for COKE2B2 in the eighth cycle.

4.2 Low-Cycle Fatigue Estimation Using Machine Learning

Various studies have been conducted to predict cyclic fatigue, and different models have been suggested (ASCE/SEI 7-10, 2010; FEMA 356, 2000). In this section, the low-cycle model is dependent on the effective stiffness (k_{eff}) and total deformation (δ_t). The log plots of both N_f and plastic deformation (δ_p) indicate linear trends until fracture or load reduction for repeated constant loading. The damage index is calculated using Eq. (2) proposed by Lee et al. (2014):

$$N_f = C^{-1}(\Delta\delta_t/k_{eff})^{-1/c}, \tag{1}$$

$$D_i = \frac{C}{2}\sum_{i=1}^{2N}(\Delta\delta_t/k_{eff})^{-1/c}, \tag{2}$$

where N_f is the number of cycles at which the fracture of the damper occurs; C is the fatigue parameter, which is dependent on the materials and load-resistance mechanism (Lee et al. 2014); δ_t is the total deformation; k_{eff} is the effective stiffness of the damper; $\Delta\delta_t/k_{eff}$ is the ratio of the total deformation for the effective stiffness of the damper; and D_i is the damage index.

In Table 4, a low-cycle fatigue damage model is presented for coke-type dampers. This model has been modified the equation by Lee et al. (2014) and the effect of the effective stiffness and total deformation change is considered and compared with that of the Manson–Coffin model. Figure 9a shows the applied load deterioration according to the number of cycles. As the number of cycles increase, the applied load significantly decreases in two cycles for COKE4B3. However, the loads for COKE4B2 and COKE4B4 fall sharply in one cycle, and the experiment is terminated after the maximum loading is achieved. Figure 9b presents the N_f estimation results of the proposed model, and the comparison of these results with the experimental results. It can be seen that the proposed estimations satisfactorily predict the fracture cycle number. Figure 9c shows the calculated damage index of each specimen using the proposed low-cycle fatigue model. As

Table 4 Low-cycle fatigue damage model

	Manson–Coffin model	Modified model
Default parameters	Plastic deformation ($\Delta\delta_p$)	Total deformation ($\Delta\delta_t$) Effective stiffness (K_{eff})
Manson–Coffin relationship	$\Delta\delta_p = 85.135(N_f)^{-0.558}$ $N_f = 2877.23(\Delta\delta_p)^{-1.792}$	$\Delta\delta_t/k_{eff} = 171.67(N_f)^{-0.558}$ $N_f = 740.74(\Delta\delta_t/k_{eff})^{-1.792}$
Half-cycle damage ($1/2N_f$)	$(1.738\times10^{-4})(\Delta\delta_p)^{1.792}$	$(6.75\times10^{-4})(\Delta\delta_t/k_{eff})^{1.792}$
Total damage index (D_i)	$(1.738\times10^{-4})\sum_{i=1}^{2N}(\Delta\delta_{pi})^{1.792}$	$(6.75\times10^{-4})\sum_{i=1}^{2N}(\Delta\delta_t/k_{eff})_i^{1.792}$

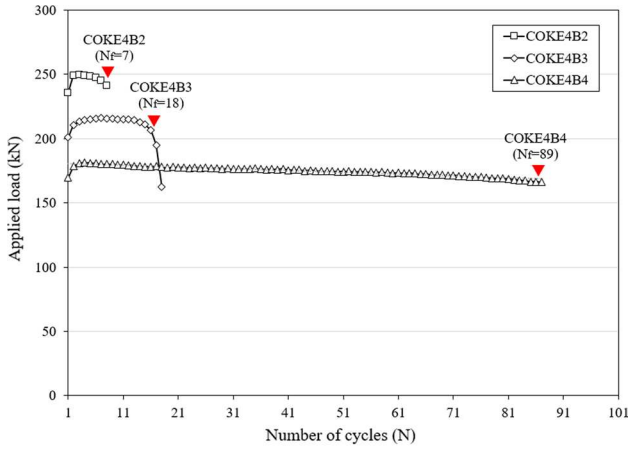

(a) Applied load deterioration with the number of cycles

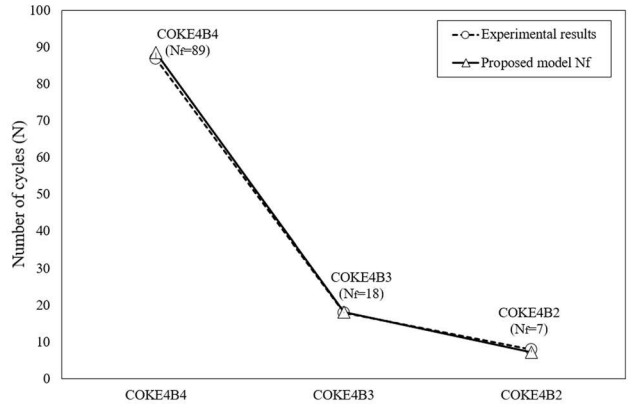

(b) N_f estimation of proposed model and comparison with the test results

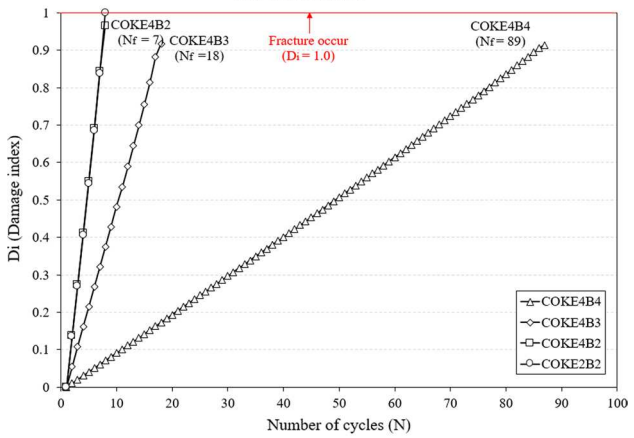

(c) Calculated damage index of each specimen

Fig. 9 Experimental result and low-cycle damage model

a verification procedure for the proposed model, Fig. 9c shows the calculated damage index of each specimen, using the proposed low-cycle fatigue model. The more reliable the model, the more the damage index (Di) reaches 1.0 when the damper fracture. When predicting the point of failure with the proposed model, the failure point was found to be higher than 1.0 for COKE2B2 and COKE4B2, while the damage index (0.91) is slightly underestimated for COKE4B3 and COKE4B4.

For long-term predictions under repeated cycles, a linear regression algorithm of machine learning is applied to estimate the damage index of fatigue resistance. Figure 10 shows the linear regression neural network model for the damage index of the fracture.

$w_0, \ldots, w_n$ represents the coefficient (parameters are energy dissipation capacity, effective stiffness, maximum strength, total deformation) of $f(x)$, y is the damage index, $\hat{y}$ represents the estimation of damage index. The holdout method (sampling) (Raschka 2015) is used to generate and test a model by dividing the training and test data. This is the most common random sampling technique, and training data (2/3) and test data (1/3) are generally used during sampling. Figure 11 compares the damage index predictions of the coke damper with those of machine learning, and shows the process of machine learning. The parameters are not only limited to the maximum strength and effective stiffness of the damper, but also include the final damage index based on the energy dissipation capacity, effective stiffness, maximum strength, and total deformation, which decrease with each cycle. Considering all the effects of multivariables, which is an advantage of machine learning, more accurate predictions can be made through linear algorithms. From the graph, it can be confirmed that the damage index result inferred from the experimental values and that obtained through the machine learning almost identical (RMSE value is 0.1).

4.3 Failure Modes

Figure 12 shows the failure mode of the COKE4B4 specimen under constant cyclic loading. For COKE4B4, small cracks start to occur at the 58th repeated cycle. After repeatedly receiving more than 63 tensile and compressive loads, the cracks gradually deepened at the expected plastic hinge location and finally fractured with a sudden load reduction beyond the 87th cycle, marking the end of the experiment. The low-cycle fatigue test of the coke damper indicates that the coke damper exhibits resistance to low-cycle fatigue with sufficient inelastic deformation beyond the 87th cycle after yielding, and the final fracture occurs at the expected plastic locations.

5 Conclusions

This study introduced coke-shaped dampers to improve damper ductility. The goal was to maximize the inelastic deformation capacity by placing multiple plastic hinges along the strip cross-section. As the in-plane resistance-type damper could cause brittle fracture following repeated cyclic loads, the fatigue performance of the damper was

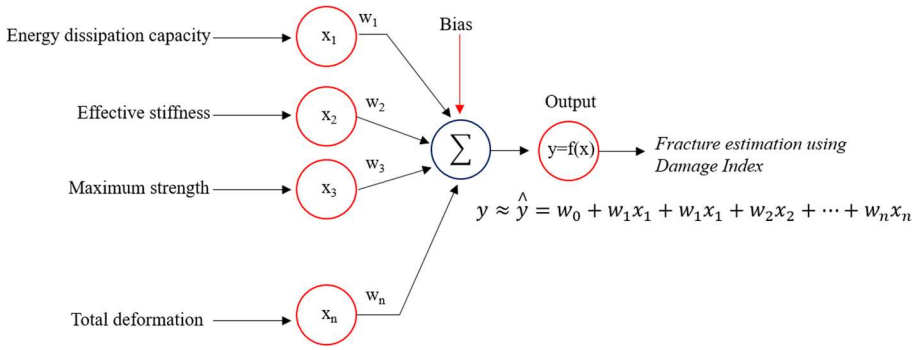

Fig. 10 Linear regression neural network model for fracture estimation

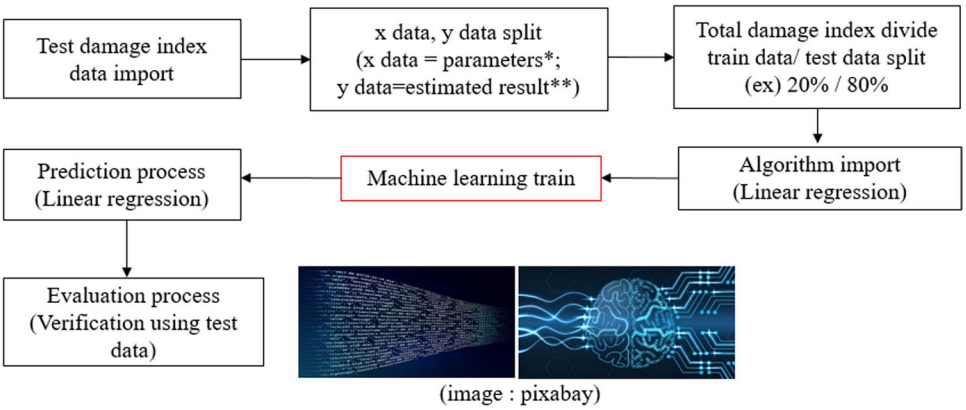

Fig. 11 Damage index predictions using machine learning (ascending order)

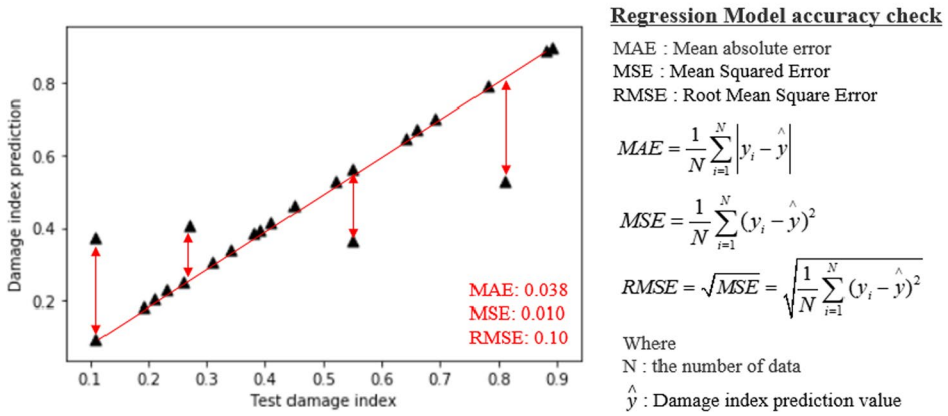

verified through a constant cyclic load test of the specimen. After constructing the damage-index model considering the total strain and effective stiffness of the fatigue test results, the damage index was predicted using a linear regression algorithm of machine learning. The following results were obtained:

1. In the test results, the proposed coke-shaped metallic damper (COKE4 and COKE2) showed stable load–displacement hysteresis behavior. The damper exhibited sufficient shear resistance capability by demonstrating a maximum strength greater than the theoretical maximum strength.
2. In the comparison of COKE4 to COKE2, the yield strength of COKE4 was found to be relatively small, and yielding started earlier than in COKE2 owing to defects in the strip. However, the final fracture of COKE2 occurred faster than that of COKE4. In summary, as the number of plastic hinges increased in a strip, the ductility of the damper increased.
3. The damage point was estimated by applying a fatigue model according to the maximum strain and effective

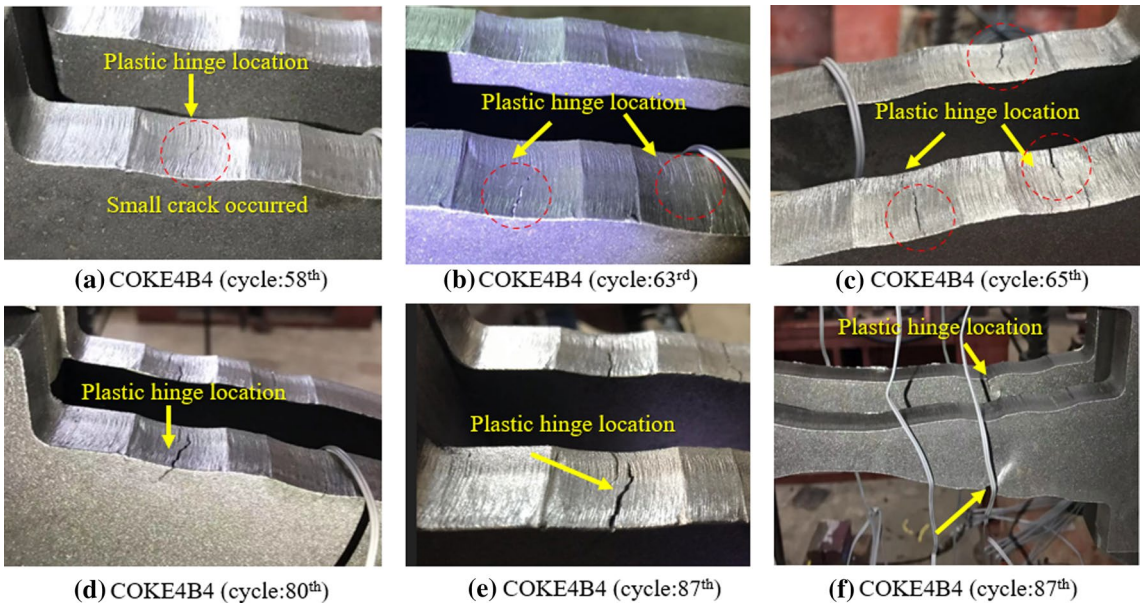

Fig. 12 Failure mode of COKE4B4 under constant load test

stiffness change. This low-fatigue model was able to predict the number of periodic failures and its results were found to be in excellent agreement with the experimental results.

4. In this study, the damage-index model from experimental results was estimated by using machine learning. The linear regression algorithm of machine learning was used for predicting the low-cycle fatigue. The results demonstrated that the predicted damage index matched the experimental damage index by more than 90%, indicating that machine learning could be used effectively for fatigue prediction.
5. This paper showed that machine learning could be used for resistance fatigue prediction because of the limitations of the test subject. It is necessary to further expand the sample set and study the effect of various variables on fatigue prediction in order to increase the reliability, in the future.

Acknowledgements This work was supported by the National Research Foundation of Korea (NRF) grant funded by the Korean government (MSIT) (NRF-2020R1A2C3005687, NRF-2018R1A4A1026027).

References

ASCE/SEI 7-10. (2010). *Minimum design loads for buildings and other structures*. Reston, VA: American Society of Civil Engineers.

Bae, J., & Karavasilis, T. L. (2018). Seismic design and assessment of steel frames with visco-plastic dampers. *International Journal of Earthquake and Impact Engineering, 2*(4), 282–297.

Chan, R. W., & Albermani, F. (2008). Experimental study of steel slit damper for passive energy dissipation. *Engineering Structures, 30*(4), 1058–1066.

Chen, G., Mu, H., & Bothe, E. R. (2001). Metallic dampers for seismic design and retrofit of bridges.

Christopoulos, C., Filiatrault, A., & Bertero, V. V. (2006). *Principles of passive supplemental damping and seismic isolation*. Pavia: IUSS Press.

Constantinou, M. C, Soong, T. T., & Dargush, G. F. (1998). Passive energy dissipation systems for structural design and retrofit.

Deng, K., Pan, P., Li, W., & Xue, Y. (2015). Development of a buckling restrained shear panel damper. *Journal of Constructional Steel Research, 106,* 311–321.

Engelhardt, M. D., Winneberger, T., Zekany, A. J., & Potyraj, T. J. (1996). The dogbone connection: Part II. *Modern Steel Construction, 36*(8), 46–55.

Fatemi, A., & Yang, L. (1998). Cumulative fatigue damage and life prediction theories: A survey of the state of the art for homogeneous materials. *International Journal of Fatigue, 20*(1), 9–34.

FEMA 356. (2000). *Prestandard and commentary for the seismic rehabilitation of buildings*. Washington, DC: Federal Emergency Management Agency.

Khazaei, M. (2013). Investigation on dynamics nonlinear analysis of steel frames with steel dampers. *Procedia Engineering*, *54*, 401–412.

Kim, Y. J., Ahn, T. S., Bae, J. H., & Oh, S. H. (2016). Experimental study of using cantilever type steel plates for passive energy dissipation. *International Journal of Steel Structures*, *16*(3), 959–974.

Krawinkler, H., & Zohrei, M. (1983). Cumulative damage in steel structures subjected to earthquake ground motions. *Computers and Structures, 16*(1–4), 531–541.

Kuroda, M. (2002). Extremely low-cycle fatigue life prediction based on a new cumulative fatigue damage model. *International Journal of Fatigue, 24*(6), 699–703.

Lee, C. H., Kim, J., Kim, D. H., Ryu, J., & Ju, Y. K. (2016a). Numerical and experimental analysis of combined behavior of shear-type friction damper and non-uniform strip damper for multi-level seismic protection. *Engineering Structures, 114,* 75–92.

Lee, C. H., Lho, S. H., Kim, D. H., Oh, J., & Ju, Y. K. (2016b). Hourglass-shaped strip damper subjected to monotonic and cyclic loadings. *Engineering Structures, 119,* 122–134.

Lee, C. H., Ryu, J., Oh, J., Yoo, C. H., & Ju, Y. K. (2016c). Friction between a new low-steel composite material and milled steel for SAFE Dampers. *Engineering Structures, 122,* 279–295.

Lee, C. H., Woo, S. K., Ju, Y. K., Lee, D. W., & Kim, S. D. (2014). Modified fatigue model for hourglass-shaped steel strip damper subjected to cyclic loadings. *Journal of Structural Engineering, 141*(8), 04014206.

Mohammadi, R. K., Nasri, A., & Ghaffary, A. (2017). TADAS dampers in very large deformations. *International Journal of Steel Structures, 17*(2), 515–524.

Oh, S. H., Kim, Y. J., & Ryu, H. S. (2009). Seismic performance of steel structures with slit dampers. *Engineering Structures, 31*(9), 1997–2008.

Raschka, S. (2015). *Python machine learning*. Birmingham: Packt Publishing Ltd.

Tamai, H., Kondoh, K., & Hanai, M. (1998). Very-low-cycle fatigue characteristics of hysteretic damper installed in K-braced frame and its life prediction under severe seismic loading. In *Proceeding of Fifth Pacific Structural Steel Conference* (Vol. 1, pp. 353–358). Seoul, Korea.

Tse, K. T., Kwok, K. C., & Tamura, Y. (2012). Performance and cost evaluation of a smart tuned mass damper for suppressing wind-induced lateral-torsional motion of tall structures. *Journal of Structural Engineering, 138*(4), 514–525.

Usami, T., Wang, C., & Funayama, J. (2011). Low-cycle fatigue tests of a type of buckling restrained braces. *Procedia Engineering, 14,* 956–964.

Zhang, C., Aoki, T., Zhang, Q., & Wu, M. (2013). Experimental investigation on the low-yield-strength steel shear panel damper under different loading. *Journal of Constructional Steel Research, 84,* 105–113.